Carrier Lifetime in Indium Antimonide*

R. A. LAFF† AND H. Y. FAN
Department of Physics, Purdue University, Lafayette, Indiana
(Received August 22, 1960)

The recombination of excess electron-hole pairs in indium antimonide has been studied in the temperature range 200°K–15°K, where it is controlled by localized centers. Minority carrier trapping is found in extrinsic p-type material. The lifetimes of electrons and holes obtained from photoconductivity and photoelectromagnetic effect data on n- and p-type samples lead to a model for the recombination, consisting of a donor center having two energy levels in the forbidden gap, at 0.055 and 0.12 ev above the valence band. The capture coefficients for holes and electrons have been determined for the center in each of the two charge states. In p-type material, the chemical acceptors are in statistical equilibrium with the free holes in the valence band. When holes freeze out onto acceptor centers ($T<60$°K), an increase of free holes due to photoexcitation leads to a corresponding increase in the hole concentration on the acceptors. This effect of majority carrier trapping reduces the rise of hole lifetime with decreasing hole concentration. In order to determine the nature of the recombination centers, different treatments are used to introduce additional centers. It is found that bombardment with 4.5-Mev electrons produces additional centers having the same recombination properties as the original centers. The result indicates that the recombination centers have the nature of structural defects rather than chemical impurities.

INTRODUCTION

PREVIOUS studies of recombination in indium antimonide[1–3] have established the existence of recombination centers which control excess carrier lifetimes at temperatures below 200°K. The centers exhibit the property of minority carrier trapping in p-type material.[3] It has been shown[2] that the assumption of a simple one-level model with temperature-independent capture rates cannot explain the observed temperature dependence of lifetimes in p-type material.

In this study, the temperature range of investigation has been extended down to 15°K. Measurements have been made on both p-type and n-type samples. The lifetimes of majority and minority carriers are deduced from steady-state photoconductivity and photoelectromagnetic effect. In the determination of lifetimes from the data, effects of carrier trapping, surface recombination, depth of light penetration, and possible presence of two types of holes have been taken into account. A model for the recombination process is deduced from the analysis of the results, and evidence is obtained that the recombination centers are due to structural defects.

EXPERIMENTAL PROCEDURES AND EQUIPMENT

Single crystals grown from zone-refined indium antimonide were used. No impurities were deliberately introduced, and the ingots were often p type at the seed end and n type at the bottom end. The samples were cut to bridge shape by using a sandblasting jig and were then etched in CP4 solution to a final thickness of ~0.3 mm. All contacts to the samples were masked to avoid photovoltaic effects. Dc measurements were made using standard potentiometer circuitry, and photoconductive measurements were made with a Perkin-Elmer amplification system with light chopped at 13 cps. The samples were isolated from ground so that measurements could be made between any pair of arms of the sample, the ground being established at whichever arm was connected to the grounded side of the high-impedance preamplifier. The light intensity was measured at the sample position in order to avoid errors due to atmospheric absorption; a Reeder thermocouple was used. Monochromatic light was provided by a Perkin-Elmer Model 98 spectrometer. The magnet used provided field strengths up to 8300 gauss and was calibrated against proton resonance.

Liquid hydrogen was used for measurements at temperatures below 77°K. A glass cell is used. The central part containing the coolant has a copper bottom to which the sample chamber was attached through a thin walled monel tubing. The temperature of the sample was controlled by the use of exchange gas in the monel tubing and a heater wound on the wall of the sample chamber. The sample chamber was surrounded with a radiation shield which was attached directly to the bottom of the coolant bath. The sample chamber and radiation shield were equipped with Mylar windows to admit the radiation used in the measurements. The bath could be pumped to obtain temperatures below the normal boiling point of the coolant, which was either liquid nitrogen or liquid hydrogen. The temperature was measured by using the sample chamber as the bulb of a constant volume helium gas thermometer.

METHODS FOR THE DETERMINATION OF LIFETIMES

Photoconductivity and Photoelectromagnetic Effect

Under a steady-state, nonequilibrium condition, a mean lifetime of excess carriers can be defined by

$$\tau=\Delta n/U, \quad (1)$$

* Work supported by an Office of Naval Research contract.
† Now at IBM Research Laboratories, Poughkeepsie, New York.
[1] G. K. Wertheim, Phys. Rev. **104**, 662 (1956).
[2] R. N. Zitter, A. J. Strauss, and A. E. Attard, Phys. Rev. **115**, 266 (1959).
[3] R. A. Laff and H. Y. Fan, Bull. Am. Phys. Soc. **2**, 347 (1957).

where Δn is the concentration of excess carriers and U is the net generation or recombination rate per unit volume. We are interested in the case where electrons and holes are generated in pairs. However, some of the excess carriers of one sign or of both signs may become trapped, leading to unequal concentrations of free excess carriers. The lifetimes defined by (1) may therefore be different for electrons and holes. The combination of two steady-state measurements may be used to determine the lifetimes of both carriers. The first of these involves the measurement of excess conductivity under illumination, the second the determination of an ambipolar diffusion length. In the case where the diffusion length is very short, it can be deduced from the photoelectromagnetic (PEM) effect. From a suitable combination of the two types of measurements, both the majority and the minority carrier lifetimes can be deduced. Photoconductivity and PEM effect have been treated[4–9] with different restrictions. In the analysis of the result, we shall take into account surface recombination and variation of light absorption in depth, without imposing the limitation of weak magnetic field. Furthermore, in indium antimonide, the structure of the valence band near the energy maximum is not known accurately and the possibility of the presence of two types of holes cannot be positively ruled out.[10] This is also taken into account. The expressions of more general validity which are used in the analysis are derived by combining the existing treatments.

The assumptions made in deriving the expressions are the following:

1. One-dimensional geometry. In order to approximate this condition, the samples used were made much wider than their thickness. End effects were eliminated by measuring voltages between probes rather than between end leads.

2. Small signal approximation. The increase of conductance of the sample was less than one percent at the highest light intensity used, usually less than 0.1%. Nonlinearity with light intensity was not observed.

3. Multiple reflection of radiation in the sample was neglected. The effect is important only at low absorption. The PEM data used are those obtained at shorter wavelengths, where the absorption coefficient is very high. From the photoconductivity data, the peak value in the spectral distribution is used in addition to the short-wavelength data. The peak occurs near the absorption edge. However, for the samples used, light intensity diminished already to 2% upon reaching the back surface, for the wavelength corresponding to the peak.

4. Same recombination velocity for front and back surfaces. This condition was verified for several samples, with both surfaces treated the same way, by making measurements with light falling first on one then on the other surface.

5. Quantum efficiency for hole-electron excitation equal to unity. Tauc[11a] found that the quantum efficiency is equal to unity at wavelengths larger than 2.5 microns. At two microns, the shortest wavelength of our measurements, the quantum efficiency was found to be slightly higher, by about 10%.

6. Sample thickness, t, large compared to ambipolar diffusion length, L. The ratio, t/L, is assumed to be large so that $\cosh(t/L)\sim\sinh(t/L)\sim 1$. For all samples used, $t/L>5$ and the assumption is justified.

7. Ratio of the two types of holes unchanged by light. The assumption is reasonable since the lifetime of holes, $\sim 10^{-7}$ sec, should be much longer than the relaxation time between two valence bands. We have then:

$$(p_2+\Delta p_2)/(p_1+\Delta p_1)=p_2/p_1=\Delta p_2/\Delta p_1. \tag{2}$$

8. Concentration ratio of excess electrons, Δn, and excess holes, Δp, remains constant in the sample. Since we wish to cover the case of carrier trapping, we do not take Δp and Δn to be equal. However, the ratio $\Delta p/\Delta n$ will be assumed to remain constant in the sample. Under steady-state conditions, the rate of recombination in any region of the sample must be the sample for electrons and holes; therefore $\Delta p/\Delta n=\tau_p/\tau_n$. For sufficiently small signal, τ_p/τ_n and hence $\Delta p/\Delta n$, remain constant. We assume also that $\Delta n/\Delta p$ is the same near the surfaces as in the bulk. In most cases, the internal consistency of the results of analysis indicates that the last assumption is justified. A case where the assumption appears to be not valid, will be pointed out later.

Under the above assumptions, the expressions obtained for the photoconductive and PEM currents, per unit sample width, are

$$i_{\mathrm{PC}}=eI_0E_x\left[\mu_n\tau_n+\left(\frac{\mu_1p_1+\mu_2p_2}{p_1+p_2}\right)\tau_p\right]F, \tag{3}$$

$$i_{\mathrm{PEM}}=eI_0\theta^*L^*G^*, \tag{4}$$

where I_0 is the density of photon flux and E_x is the applied electric field. The factor F in (4) is the ratio of i_{PC} to the ideal current which is expected when there are no surface recombination and no transmitted radiation. It is given by

$$F=\frac{1-\exp(-\alpha t)}{1+S}+\frac{S}{1+S}\left[\frac{1}{1+\alpha L}-\frac{\exp(-\alpha t)}{1-\alpha L}\right], \quad \alpha L\neq 1; \tag{5}$$

$$F=\frac{1}{2}\left(1+\frac{1}{1+S}\right), \quad \alpha L=1.$$

[4] W. van Roosbroeck, Phys. Rev. **101**, 1713 (1956).
[5] S. W. Kurnick and R. N. Zitter, J. Appl. Phys. **27**, 278 (1956).
[6] W. Gartner, Phys. Rev. **105**, 823 (1957).
[7] R. N. Zitter, Phys. Rev. **112**, 852 (1958).
[8] A. Amith, Phys. Rev. **116**, 793 (1959).
[9] A. K. Walton and T. S. Moss, Proc. Phys. Soc. (London) **73**, 399 (1959).
[10] G. W. Gobeli and H. Y. Fan, Phys. Rev. **119**, 613 (1960).
[11a] J. Tauc, J. Phys. Chem. Solids **8**, 219 (1958).

The factor G^* is the ratio of the actual PEM current to the ideal PEM current which would be obtained under the following conditions: no surface recombination, no transmitted radiation, sample thick compared to diffusion length, and diffusion length much larger than the reciprocal absorption coefficient, α^{-1}. Under the approximations made, it is given by

$$G^*=\frac{1}{1+S^*}\left[\frac{\alpha L^*}{1+\alpha L^*}-\frac{\alpha L^*}{1-\alpha L^*}\exp(-\alpha t)\right], \quad \alpha L^*\neq 1;$$
$$G^*=\frac{1}{2}\left(\frac{1}{1+S^*}\right), \quad \alpha L^*=1. \tag{6}$$

The factor S is defined by

$$S=\tau_n s_n/L, \tag{7}$$

where s_n is the surface recombination velocity for electrons and L is the ambipolar diffusion length. The superscript asterisk refers to quantities under the applied magnetic field.

$$L^*=\left\{\frac{kT}{e}\mu_n^*\left(\frac{p_1\mu_1^*+p_2\mu_2^*}{p_1+p_2}\right)\times\left[\frac{(p_1+p_2)\tau_n+n\tau_p}{p_1\mu_1^*+p_2\mu_2^*+n\mu_n^*}\right]\right\}^{\frac{1}{2}}, \tag{8}$$

where

$$\mu^*=\mu\frac{\langle\tau_s/(1+\omega^2\tau_s^2)\rangle}{\langle\tau_s\rangle}, \tag{9}$$

$$\omega=eB/m^*, \tag{10}$$

and τ_s is the relaxation time for scattering. The PEM angle, θ^*, in (4) is given by

$$\theta^*=B\left[\mu_n{}^H\frac{\mu_n{}^{**}}{\mu_n{}^*}+\frac{\mu_1{}^H\mu_1{}^{**}p_1+\mu_2{}^H\mu_2{}^{**}p_2}{\mu_1{}^*p_1+\mu_2{}^*p_2}\right], \tag{11}$$

where μ^H is the zero-field Hall mobility and

$$\mu^{**}=\mu\frac{\langle\tau_s^2/(1+\omega^2\tau_s^2)\rangle}{\langle\tau_s^2\rangle}. \tag{12}$$

In (9) and (12) the bracketed quantities denote averages taken over a Maxwellian energy distribution.

The above expressions may be used to determine the mean lifetimes τ_n and τ_p if the mobilities and carrier concentrations are known. One procedure is as follows: As shown in Fig. 1, which gives the data for a typical sample, the photoconductivity goes through a maximum with decreasing wavelength and increasing absorption coefficient. The maximum is predicted by (5) with nonvanishing S, as αL varies from values much less than unity to values much greater than unity. In Fig. 2, F is plotted as a function of $(1/\alpha L)$ for two different

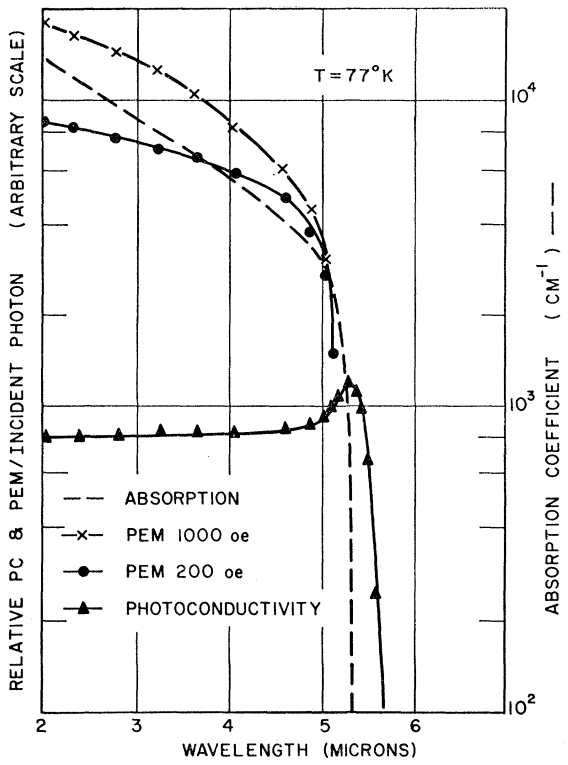

FIG. 1. Wavelength dependence of photoconductivity, PEM current and absorption coefficient.

values of $W=t/L$ and various values of S. If $W>5$, F attains a maximum value greater than 0.5 even in the case of an infinite surface recombination velocity. For most of the samples measured, $S\ll 5$, $W>10$. Under such conditions, the peak value of F is greater than 0.75. On the other hand, $F\rightarrow(1+S)^{-1}$ at short wavelengths where $\alpha L\gg 1$. Hence an estimate of S can be obtained from the ratio of the photoconductivity at the maximum to that at short wavelengths. For $\alpha L\gg 1$, the factor $G=G^*(B=0)$ of the PEM effect also reduces to $(1+S)^{-1}$. All samples measured had $\alpha L>7$ at the wavelength of 2 microns, so that $G>\frac{7}{8}[1/(1+S)]$ at that wavelength. Thus, having obtained S from the wavelength dependence of photoconductivity, we can get estimates of both F and G. With knowledge of I_0, both τ_n and τ_p can be determined from (3), (4), (8), and (11).

The above method does not require accurate knowledge of the wavelength dependence of absorption coefficient or of PEM effect. A second method is to determine the value of L by using (6) and the data on the variation of PEM current with absorption coefficient. Equation (8) provides then one equation for τ_n and τ_p. Another equation is obtained by taking the ratio of (3) and (4). Using short-wavelength data for which $F\sim G\sim(1+S)^{-1}$, the factors F and G as well as the radiation intensity, I_0, are eliminated in the process. The two equations can be used to obtain τ_n and τ_p. The

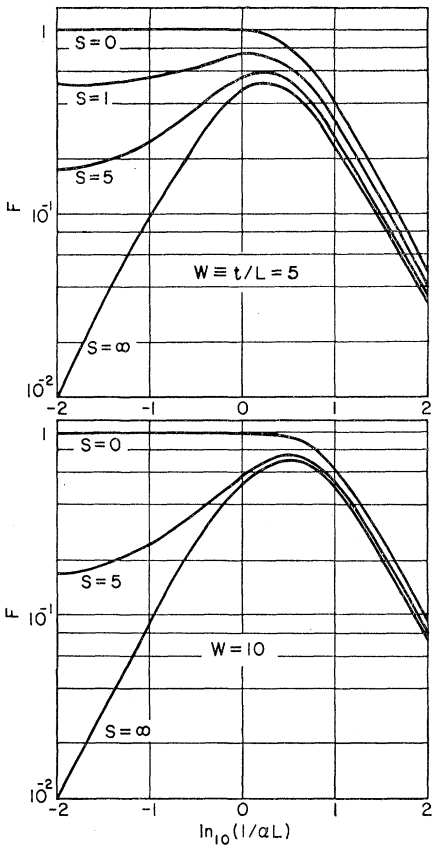

FIG. 2. Calculated dependence of the factor F of photoconductivity as a function of $\ln(1/\alpha L)$ with the surface recombination factor, S, as a parameter, for two values of the ratio, W, of sample thickness, t, to diffusion length, L.

results calculated by the two different methods give a check of self-consistency of the data and the interpretation.

Application to Different Types of Samples

The deduction of lifetime from photoconductivity and PEM data requires the knowledge of the carrier concentrations and mobilities which enter (3), (4), (8), and (11). We now consider individually extrinsic p-type, extrinsic n-type, and near intrinsic samples.

In p-type material, the effective hole mobility in (3) can be determined from the product of the conductivity and the Hall coefficient in the limit of high field. The Hall mobility of electrons, $\mu_n{}^H$, is needed in (11). Since the electron mobility in InSb is very much higher than the hole mobility, the contribution to (11) from the holes is quite small at low magnetic field strengths. At high magnetic field strengths, the relative contribution due to holes becomes larger, due to higher magnetoresistive effect of electrons as compared to that of holes, but at the fields employed in these experiments, the electrons still dominate the PEM angle. The drift mobility and the concentration of electrons are needed in (8). The drift mobility is also needed in (3). For highly p-type material, with $n \ll p$,

$$n\tau_p \ll p\tau_n, \tag{13a}$$

$$n\mu_n{}^* \ll (p_1\mu_1{}^* + p_2\mu_2{}^*). \tag{13b}$$

Equation (8) then reduces to the effective electron diffusion length,

$$L_n{}^* = [(kT/e)\mu_n{}^*\tau_n]^{\frac{1}{2}}, \tag{14}$$

and the electron concentration is no longer needed. The electron mobilities are determined from the magnetic field dependence of PEM effect at short wavelengths, a method first used by Kurnick and Zitter.[5] In agreement with their conclusions, we find that the approximation, $\mu_n = \mu_n{}^H$ and $\mu_n{}^* = \mu_n{}^{**}$, corresponding to an energy-independent relaxation time, seems to give satisfactory agreement with the measured results. The temperature dependence of electron mobility determined by this method is shown in Fig. 3 for two p-type samples (curve A). At temperatures above 200°K, the electron mobility can be determined from Hall coefficient and conductivity. The three points at the high-temperature end of curve A were so obtained. They fall on a smooth curve with the rest of the points. Also shown (curve B) is the Hall mobility of electrons for an n-type sample from the same ingot. Comparison of the two curves also indicates that the electron

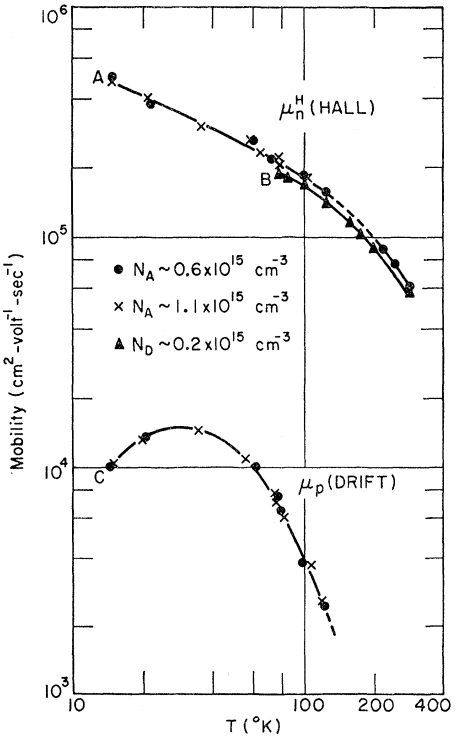

FIG. 3. Temperature dependence of mobilities. Curves A and C are, respectively, electron and hole mobilities in two p-type samples. Curve B is the Hall mobility of electrons, measured at 700 gauss, in an n-type sample from the same ingot.

mobility obtained from the PEM effect is reasonable. The hole mobilities of the same two samples are shown in curve *C*.

In *n*-type samples, the photoconductivity is determined mainly by the majority carriers, due to the large ratio of electron to hole mobility. Only the majority carrier mobility, μ_n, is needed to determine the electron lifetime, τ_n, from (3). Combining (8), (11), and (4), we obtain in the limit of small magnetic field

$$i_{\mathrm{PEM}}/BeI_0 \sim \mu_n{}^H\left[\frac{kT}{e}\tau_p\left(\frac{p_1\mu_1+p_2\mu_2}{p}\right)\right]^{\frac{1}{2}}G. \quad (15)$$

Using the hole mobility obtained for the *p*-type samples as an estimate of hole mobility, we find from (15) values of τ_p for the *n*-type samples which are close to the values of τ_n. There does not seem to be appreciable trapping of minority carriers in the *n*-type samples.

Near-Intrinsic Range

There is no special problem as *n*-type samples become nearly intrinsic. In *p*-type samples the Hall coefficient reverses its sign in the near intrinsic range. When (13) ceases to be valid because of the increase of electron concentration, the complete expression (8) for L^* has to be used. Therefore n/p will be needed, in addition to the hole and electron mobilities. The electron mobility can be obtained by interpolation between low and high temperatures, as in curve *A* of Fig. 3. We have used the following methods to calculate both τ_n and τ_p for the temperatures of Hall reversal and maximum negative Hall coefficient, and to calculate τ_n for higher temperatures.

At the Hall reversal, condition (13b) still holds. We assume that condition (13a) holds also, and calculate τ_n and τ_p in the same way as for the extrinsic region. The assumption is verified by getting μ_p from extrapolation of the extrinsic data and estimating (n/p) approximately from the condition $n/p \sim (\mu_p/\mu_n)^2$. For our samples, the values of (τ_n/τ_p) and the values of (n/p) so obtained are found to satisfy actually the condition (13a).

At the maximum of negative Hall coefficient, condition (13b) no longer holds. In fact, it can be easily shown that, with an electron mobility much higher than the hole mobility, we have at this point

$$n\mu_n \sim (p_1\mu_1+p_2\mu_2). \quad (16)$$

Therefore (8) reduces to

$$L=\left(\frac{kT}{e}\mu_n\tau_n\right)^{\frac{1}{2}}\left(\frac{1+n\tau_p/p\tau_n}{2}\right)^{\frac{1}{2}}, \quad (17)$$

in the case of small magnetic field. We assume that (13a) still holds and calculate τ_n and τ_p by the same procedure as for the extrinsic range. The assumption is justified by the fact that, for our samples, the calculated values gives

$$\mu_n\tau_n \gg [(\mu_1p_1+\mu_2p_2)/p]\tau_p, \quad (18)$$

which leads to the assumed condition (13a) in view of (16). The relation (18) indicates that the photoconductivity at this temperature is given primarily by the electrons. This will be even more so with increasing temperature and increasing ratio of electron to hole concentration. Therefore, above the temperature of negative Hall maximum, τ_n can be obtained directly from the photoconductivity but τ_p cannot be obtained reliably.

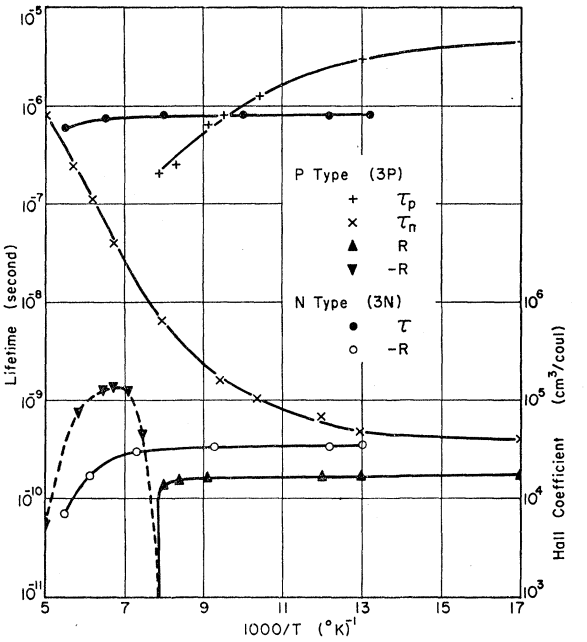

FIG. 4. Temperature dependence of lifetimes and Hall coefficient of an *n*-type and a *p*-type sample.

INTERPRETATION OF RESULTS ON LIFETIME

Model for Recombination

Measurements of lifetime have been carried out on several *p*- and *n*-type samples, according to the methods outlined above. The temperature dependence of electron and holes lifetimes are shown in Fig. 4 for a typical *p*-type and a typical *n*-type samples from the same ingot. The large ratio τ_p/τ_n in the *p*-type sample at low temperatures shows strong trapping of electrons indicating the presence of donor-type centers. At the high-temperature end of the range, both electron and hole lifetimes are about the same. Shown as a dashed curve in Fig. 5 is the attempt to fit the *p*-type data with the model of a set of recombinations centers having a single level located below the center of the energy gap. The concentration of centers is found to be 8×10^{13} cm^{-3} from the temperature variation of Hall coefficient in the exhaustion range shown in Fig. 6. The capture coefficients for electrons and holes are assumed to be

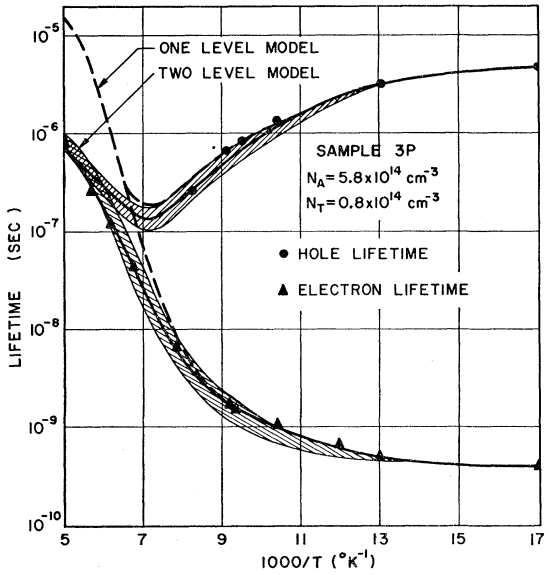

FIG. 5. Temperature dependence of electron and hole lifetimes in a p-type sample. The dashed curve and solid curves are calculated on the basis of one and two level recombination centers, respectively.

temperature independent. In agreement with Zitter, Strauss, and Attard,[2] we find that a single-level model with temperature-independent capture coefficients is inadequate to explain the p-type results over the entire temperature range. Those authors have shown that neither of the direct interband processes, photon-emissive and Auger recombinations, could account for the observed discrepancy. In addition, we find that the discrepancy cannot be attributed to a large temperature variation of the hole capture coefficient in the near intrinsic region if the recombination centers in the n-type sample from the same ingot are of the same nature, since the n-type data indicates that the capture coefficient must be essentially constant. Aside from the difficulty in fitting the p-type sample data over the whole range, the model requires that the n-type sample must have a quite different type or a much higher concentration of centers; with the same type of centers, the concentration in the n-type sample would have to be 26 times larger.

The data for the various p- and n-type samples can be interpreted on the basis of a set of recombination centers with two energy levels. As mentioned before, the centers appear to be donors in character. It is assumed that each center can be electrically neutral, singly charged, or doubly charged. The center is then characterized by six parameters: E_1, r_{c1}, r_{v1}, E_2, r_{c2}, r_{v2}, where E_1 and E_2 are the two energy levels, r_{c1} and r_{v1} are the electron and hole capture coefficients of the first level, r_{c2} and r_{v2} are the coefficients of the second level. The general problem of multilevel recombination centers has been treated before.[11] Expressions for the carrier lifetimes, which are used in our analysis, can be derived in a straightforward way. Let f_m be the probability for the center to be in the mth charged condition[12]:

$$f_m=\frac{g_m \exp[(m\zeta-\epsilon_m)/kT]}{\sum_m g_m \exp[(m\zeta-\epsilon_m)/kT]}, \tag{19}$$

where g_m is the degeneracy of the state, ϵ_m is the energy required to hold m electrons on the center, and ζ is the Fermi level. To be definite, we take $g_0=1$ and $g_1=g_2=2$, assuming that both the first and the second electrons trapped on the center have a choice of spin. Then

$$\begin{aligned} F_2&=\frac{f_2}{f_2+f_1}=\left[1+\exp\left(\frac{E_2-\zeta}{kT}\right)\right]^{-1}, \\ F_1&=\frac{f_1}{f_0+f_1}=\left[1+\tfrac{1}{2}\exp\left(\frac{E_1-\zeta}{kT}\right)\right]^{-1}. \end{aligned} \tag{20}$$

With a concentration N of such centers, the ratio of the carrier lifetimes is given by:

$$\frac{\tau_p}{\tau_n}=\left\{1+\frac{N}{p}\left[\frac{r_{c1}}{r_{v1}}\frac{A_1}{B_1}(1-F_1)+\frac{r_{c2}}{r_{v2}}\frac{A_2}{B_2}(1-F_2)\right]\right\} \times\left[1+\frac{N}{p}\left(\frac{A_1}{B_1}F_1+\frac{A_2}{B_2}F_2\right)\right]^{-1}, \tag{21}$$

and the electron lifetime is given by:

$$\tau_n=\left[N\left(1+\frac{n\tau_n}{p\tau_p}\right)\right]^{-1}\left[\frac{r_{c1}}{B_1}+\frac{r_{c2}}{B_2}\right]^{-1} \times\left[\frac{1-F_2(1-F_1)}{(1-F_1)(1-F_2)}\right], \tag{22}$$

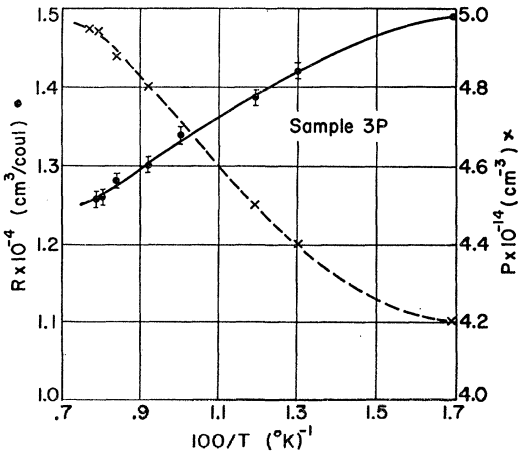

FIG. 6. Temperature dependence of Hall coefficient and hole concentration in the exhaustion range of a p-type sample.

[11] C. T. Sah and W. Shockley, Phys. Rev. **109**, 1103 (1958).

[12] H. Y. Fan, Suppl. Nuovo cimento **7**, 661 (1958).

where

$$A_1=(1-F_1)(1-F_2^2)/[1-F_2(1-F_1)]^2,$$

$$A_2=(2-F_1)(1-F_2)F_1/[1-F_2(1-F_1)]^2,$$

$$B_i=1+\left(\frac{1-F_i}{F_i}\right)\frac{nr_{ci}}{pr_{ci}}.$$

Equations (21) and (22) are used for the analysis of the data.

In p-type samples, the Fermi level is quite low at low temperature and the probability, f_2, for the center to hold two electrons is very small. Hence, the four parameters, N, E_1, r_{c1}, and r_{v1}, can be determined from the low-temperature data on the p-type sample, as in the case of one level model. On the other hand, in an n-type sample, the centers have a high probability of each holding two electrons, and the carrier lifetimes are determined primarily by Nr_{v2}, as in the one-level model. Assuming that the concentration, N, of centers in the n-type samples is the same as that in the p-type sample from the same ingot, we get the value of r_{v2} from the data on the n-type sample. The value of E_2 is chosen to fit the data on the p-type sample at 200°K. At this temperature, the lifetimes are not sensitive to the value of r_{c2}. The shaded area in Fig. 5 shows the narrow range of the calculated lifetimes for a variation of the value of r_{c2} by a factor of 100. The values of the parameters determined are:

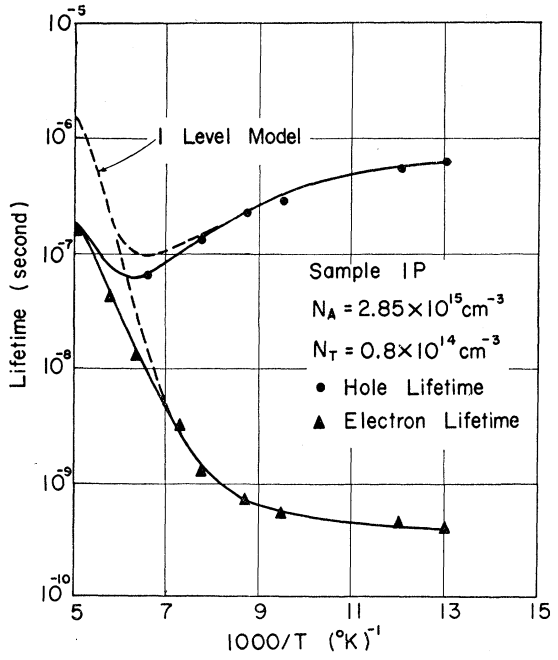

FIG. 7. Temperature dependence of electron and hole lifetimes in a p-type sample. The dashed and solid curves are calculated on the basis of one level and two level recombination centers, respectively.

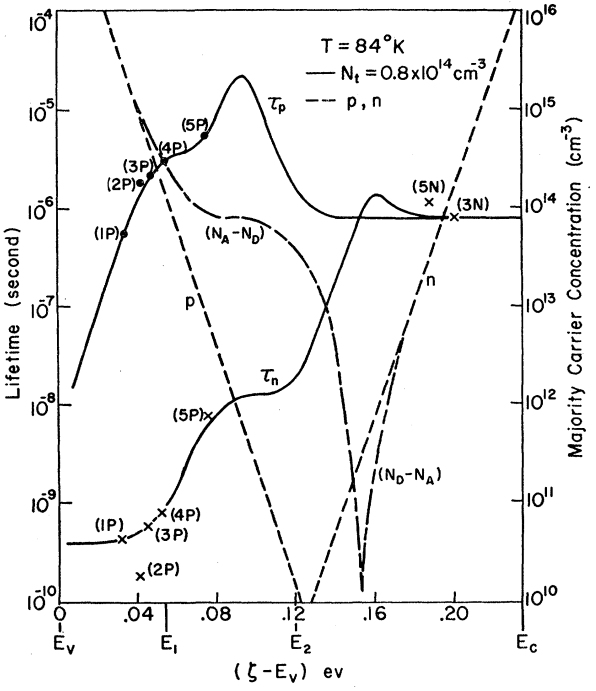

FIG. 8. Fermi-level dependence of electron and hole lifetimes for n- and p-type samples of various carrier concentrations. Solid curves are carrier lifetimes calculated by using the model of two level centers. The dashed curves show the variations of the carrier concentration, p or n, and effective impurity concentration, (N_A-N_D) or (N_D-N_A).

$$\begin{aligned} &E_1-E_v=0.055 \text{ ev}, && r_{c1}=32\times10^{-6} \text{ cm}^3 \text{ sec}^{-1},\\ &r_{v1}=6\times10^{-10} \text{ cm}^3 \text{ sec}^{-1}, && E_2-E_v=0.12 \text{ ev},\\ &r_{c2}=1.2\times10^{-6} \text{ cm}^3 \text{ sec}^{-1}, && r_{v2}\simeq10^{-8} \text{ cm}^3 \text{ sec}^{-1},\\ &&& N=0.8\times10^{14} \text{ cm}^{-3}. \end{aligned} \tag{23}$$

Another p-type sample, (1P), of higher impurity concentration which was cut from a different ingot was measured over the temperature range 200°K to 78°K. Figure 7 shows that the data can be closely fitted by the model of two-level centers with the same values for the parameters, including the concentration of centers. The hole and electron lifetimes determined at 84°K are plotted as functions of the Fermi level in Fig. 8 for several n- and p-type samples of various carrier concentrations. The samples were taken from three different ingots: (5N) and (5P) from one ingot, (1P) from another, and the rest from a third ingot. The solid curves give the lifetimes calculated by using the values (23). The general agreement between the experimental data and the calculated curves indicate that the samples have the same type of centers in comparable concentrations. The data for sample (2P) which was cut from near the seed of the pulled crystal show significant departure from the curve, particularly with respect to τ_n which is too low by a factor of three. The departure can be accounted for by a proportionately larger concentration of centers. This was con-

firmed by the analysis of the temperature dependence of the hole concentration in this sample, which actually gave a concentration of 2.4×10^{14} cm^{-3} of centers.

Consider the photoconductive response of n- and p-type samples on the basis of the curves of τ_n and τ_p. The fractional change of sample conductance per unit power of incident radiation, $\Delta G_s/G_sI$, is a measure of the sensitivity of photoresponse. Referring to (3), we can write:

$$\frac{1}{I}\frac{\Delta G}{G}\propto\left(\frac{\mu_p\tau_p+\mu_n\tau_n}{\mu_p p+\mu_n n}\right)F, \tag{24}$$

where μ_p stands for the effective hole mobility and the factor F represents the effect of surface recombination. With a mobility ratio of $\mu_n/\mu_p\sim40$ at 84°K, the quantity in brackets is dominated by holes for $\zeta<0.12$ ev and by electrons for $\zeta>0.14$ ev. It has a sharp maximum at $\zeta\sim0.1$ ev which corresponds to p-type samples of high resistivity. With increasing hole concentration or decreasing ζ, its value drops rapidly both on account of decreasing τ_p and on account of increasing p. Compensated samples having $p\sim5\times10^{12}$ cm^{-3} have been used in this laboratory as sensitive infrared detectors.

Low-Temperature Results

Measurements on two p-type samples, $2P$ and $3P$, have been extended below liquid nitrogen temperature, down to ~15°K. The results on both samples were similar. The carrier lifetimes of sample $3P$ are shown in Fig. 9. Also shown is the Hall coefficient of the sample. Below 50°K, the holes begin to freeze out on the acceptor impurities and the Hall coefficient rises. Under illumination, the production of excess free holes leads to an increase of bound holes on the acceptors since the free and bound holes are in statistical equilibrium under steady-state conditions. Thus we have the trapping of majority carriers which requires additional consideration. At low temperature, the Fermi level is close to the valence band and the recombination centers are essentially empty of electrons. Excited electrons are quickly trapped, producing a concentration Δn_t on the centers. The rate of recombination is then limited almost entirely by the capture of holes which is a much slower process. The net recombination rate for this case is

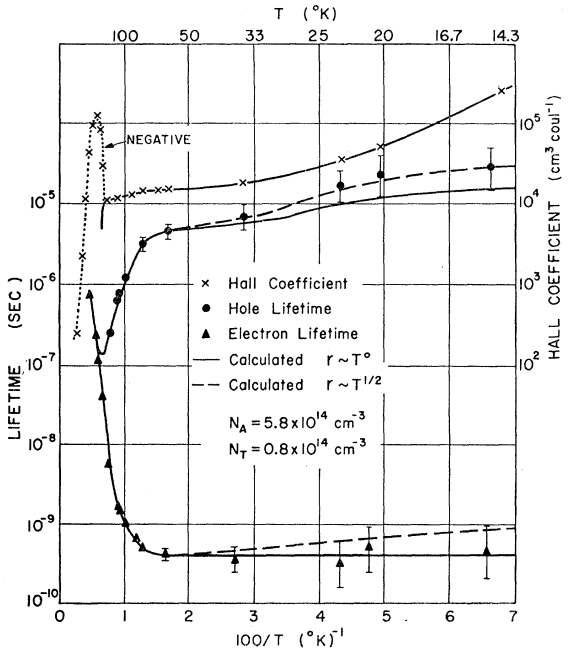

FIG. 9. Carrier lifetimes and the Hall coefficient of a p-type sample as functions of reciprocal temperature.

$$U\sim r_{v1}p\Delta n_t, \tag{25}$$

and the lifetime for holes is given by

$$\tau_p=\frac{\Delta p}{U}=\frac{1}{r_{v1}p}\frac{\Delta p}{\Delta n_t}. \tag{26}$$

The expression is a generalization of the familiar expression for the carrier lifetime at low temperature. In the absence of freezeout of majority carriers, $\Delta p\sim\Delta n_t$, when $\tau_p\gg\tau_n$. When there is an increase of bound holes, Δp_A, on the acceptor impurities the neutrality condition gives $\Delta n_t\sim\Delta p+\Delta p_A$. Thus

$$\tau_p=\frac{1}{r_v p}\frac{\Delta p}{\Delta p+\Delta p_A}. \tag{27}$$

It is easily shown that hole trapping by the acceptors does not influence the electron lifetime. The lifetime is given by

$$\tau_n=1/r_c N_t, \tag{28}$$

just as in the absence of freezeout.

The ratio $\Delta p/\Delta p_A$ can be obtained by differentiating the dissociation equation for holes:

$$\frac{p(N_A-p_A)}{p_A}=\frac{N_v}{g_A}\exp(-E_A/kT), \tag{29}$$

where p_A is the concentration of bound holes or neutral acceptors. Substituting the result in (27), we get

$$\tau_p=\frac{1}{r_v p}\frac{N_A p}{N_A p+(N_A-p_A)p_A}. \tag{30}$$

In view of the relation,

$$p_A=N_A-N_D-p, \tag{31}$$

we can write

$$\tau_p=\frac{1}{r_v p_{ex}}\left[1-\left(1-\frac{p}{p_{ex}}\right)^2\left(1-\frac{N_D}{N_A}\right)\right]^{-1}, \tag{32}$$

where $p_{ex}=N_A-N_D$ is the hole concentration in the exhaustion range where both the acceptors and com-

pensating donors are completely ionized. Assuming that the doubly charged recombination centers are the only compensating donors, i.e., $N_D=2N$, we obtain the solid curves shown in Fig. 9. The calculated curve of hole lifetime falls somewhat below the experimental curve. The discrepancy increases with decreasing temperature. The discrepancy would be larger if the presence of other compensating donors is assumed. In the calculation, the recombination coefficients r_{c1} and r_{v1} are assumed to be temperature independent. The dashed curves are computed under the assumption that r_c and r_v vary as the thermal velocity, i.e., the capture cross sections are constant. This calculation gives good fit for τ_p but the curve for electron lifetime appears to be too high at low temperature. The accuracy of the experimental results is not sufficient to decide whether either of the two assumptions is entirely correct. We note that the temperature dependence might be different for r_{c1} and r_{v1}. According to the model, at low temperature the electrons are captured with the help of double positive charge on each center, while the holes are captured against the repulsion of the single positive charge that remains after the center has captured an electron.

An interesting point was brought out in the low-temperature study. In the derivation of the expressions for photoconductivity and PEM effect, the assumption is made that the ratio of excess holes to excess electrons is the same at the surfaces as in the bulk. This assumption was apparently violated near the low-temperature end of the range of measurement. Figure 10 shows the photoconductivity curves for sample $3P$ at three temperatures. As discussed previously, the ratio of short-wavelength to peak photoconductivity gives an estimate of the surface recombination factor $1/(1+S)$. We get $S\sim4$ from the curve for 15°K. On the other hand, the surface recombination can be determined from PEM effect. From the wavelength dependence of the PEM current at small magnetic field, which corresponds to the variation of the factor G with the absorption coefficient α, we can determine the diffusion length, L, by using the relation (6). Knowing the value of L and the measured value of i_{PEM}/I_0, we can obtain the value of S from (4) and (6). This method gives a value of $S<1$ which is not consistent with the estimate obtained from the photoconductivity. We suggest that the smaller estimate of S as given by the PEM effect is closer to the correct value. The large ratio of peak to short-wavelength photoconductivity may be explained by assuming that the trapping of excess holes on the acceptor impurity is stronger at the surface than in the bulk material. According to (27) the trapping reduces the lifetime of holes by the factor $\Delta p/(\Delta p+\Delta p_A)$. The hole lifetime, τ_p, would have increased proportionately with $1/p$ in the freezeout range, much faster than the data shown in Fig. 9, if not for the effect of trapping. With a stronger trapping near the surface, the photoconductivity at short wavelengths with carriers excited near the surface will be lowered relative the peak of photoconductivity at which the radiation begins to penetrate deeply into the sample. Thus the ratio of peak to short-wavelength photoconductivity may be large without high surface recombination.

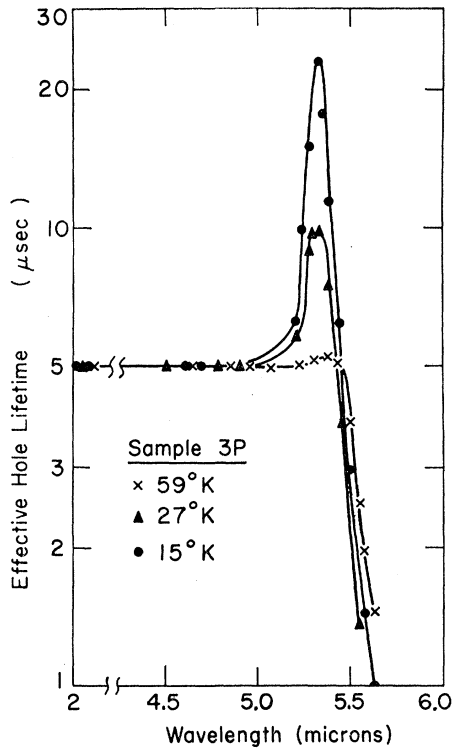

FIG. 10. Spectral dependence of photoconductivity at low temperatures.

The postulated intensification of hole trapping at the surface could be the result of potential variation near the surface. Let us suppose that the Fermi level at the surface is kept fixed relative to the energy bands by the surface states. As the Fermi level in the bulk material approaches the valence band with decreasing temperature, the energy bands will be depressed near the surface. As a result, the trapping of holes by acceptors will be stronger at the surface than in the bulk, since the energy level of acceptors near the surface is lower relative to the Fermi level. This effect tends to decrease the hole lifetime near the surface. On the other hand, the depression of the valence band reduces the hole concentration at the surface, thereby tending to increase the hole lifetime. By differentiating (30) with respect to the Fermi level, we find that the net result is to decrease τ_p at the surface if

$$\frac{2p_A}{N_A}>1+2\frac{\Delta p}{\Delta p_A}.$$

An estimate of the values of p_A/N_A and $\Delta p/\Delta p_A$ shows

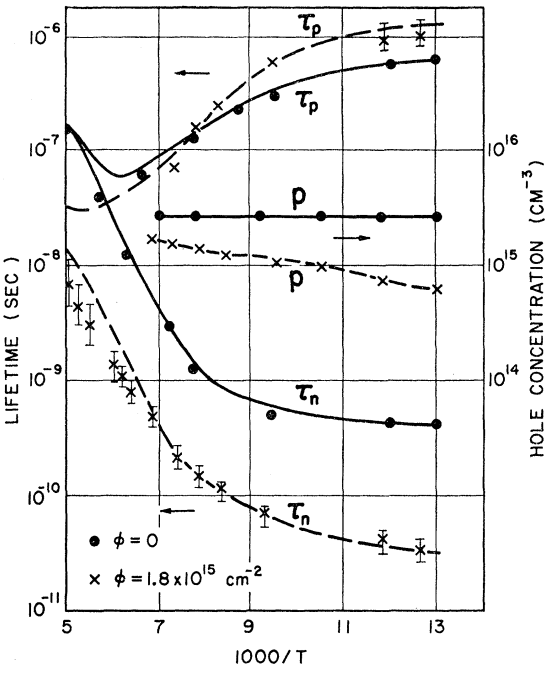

FIG. 11. Effect of 4.5-Mev electron bombardment on the lifetime and carrier concentration in the p-type sample $1P$. The points are data obtained before the bombardment and the crosses are data obtained after the bombardment.

that this condition could indeed be satisfied at the low temperature.

NATURE OF THE RECOMBINATION CENTERS

In order to determine the nature of the defects which contol the recombination, experiments have been performed to deliberately introduce defects of known types. Two methods have been tried. They are: (1) heat treatment and quenching, with and without introduction of copper, and (2) bombardment with 4.5-Mev electrons.

Two samples, intermediate between samples $2P$ and $3P$, were quenched into liquid nitrogen after heating to 435°C for 1.5 hours. One of the samples had been plated with copper. The samples were each sealed into a tube containing helium gas. After treatment, the samples were ground down and etched to remove surface disturbances. Both samples showed an increase in net acceptor concentration, the sample which was quenched without copper showing an increase of 6×10^{15} cm^{-3} net acceptors, the copper plated sample showing an increase of 1.1×10^{16} cm^{-3}. Similar results were obtained with two more samples, quenched from 340°C, except that both samples showed an increase of about 1.5×10^{14} cm^{-3} net acceptors, indicating that the copper did not diffuse efficiently at the lower temperature. Since the heat treatments increased the concentration of net acceptors, they are not helpful for the identification of the recombination centers which are of donor type.

The experiments of Aukerman[13] showed that bombardment with 4.5-Mev electrons at 200°K introduced a donor level at 0.048 ev above the valence band, along with other levels. There was also evidence that with warming to higher temperatures more acceptor defects than donor defects were annealed out. It was therefore decided to perform the bombardment at 0°C. It was desired to introduce sufficient centers for the lifetime to be dominated by these centers, but not to decrease the hole concentration so much as to raise the Fermi level at low temperature above the 0.048-ev level. Sample $1P$ was chosen for the bombardment. The thickness of the sample was much thinner than the range, so that the irradiation was uniform in depth. The resulting changes in carrier concentration and lifetime after a bombardment of 1.81×10^{15} electrons per cm^2 are shown in Fig. 11. The electron lifetime has been reduced more than an order of magnitude. The lifetime of holes has changed less drastically, as is expected from the fact that hole lifetime is relatively insensitive to trap concentration. The lifetimes and carrier concentration after bombardment were both consistent with the introduction of 1.17×10^{15} cm^{-3} additional centers of the same kind as the original centers which had a concentration of 8×10^{13} cm^3. If other centers were also introduced by the bombardment, they were apparently not effective for recombination in this temperature range. The dashed curves for lifetime and carrier concentration are computed using the two-level model for a total concentration of 1.25×10^{15} cm^{-3}. There is some discrepancy between the experimental and calculated lifetimes in the near-intrinsic region. This discrepancy is not to be regarded as too serious, because the lifetime was difficult to measure accurately in this region where the sample resistance is an order of magnitude smaller than that of unbombarded samples. The bombardment experiment leads us to believe that the common recombination centers in indium antimonide are lattice defects of a relatively simple nature.

[13] L. W. Aukerman, Phys. Rev. **115**, 1125 (1959).